Original Article | Open Access

Science Orthopedics

Wang *et al. Sci Orthop.* 2026;1:3 **DOI:**10.20517/so.2026.06

The expression characteristics of LBP in spinal tuberculosis and its regulatory effect on the TLR4/NF-κB inflammatory pathway

Jiong Wang[1,2,#], Caili Lou[1,3,#], Jian Liu[1], Hongbao Ma[1], Hekun Liu[1,2], Zhiyun Shi[4], Xu Zhang[5,‡], Ningkui Niu[1,6,‡]

Keywords:
Spinal tuberculosis, proteomics, lipopolysaccharide-binding protein, TLR4/NF-κB, inflammation

Citation: Wang J, Lou C, Liu J, Ma H, Liu H, Shi Z, Zhang X, Niu N. The expression characteristics of LBP in spinal tuberculosis and its regulatory effect on the TLR4/NF-κB inflammatory pathway. *Sci Orthop.* 2026;1:3. https://dx.doi.org/10.20517/so.2026.06

Received: 31 Mar 2026
First Decision: 21 Jul 2026
Revised: 4 Aug 2026
Accepted: 26 Aug 2026
Published: 15 Sep 2026

Academic Editor:
Zhijian Wei
Copy Editor:
Shu-Yuan Duan
Production Editor:
Shu-Yuan Duan

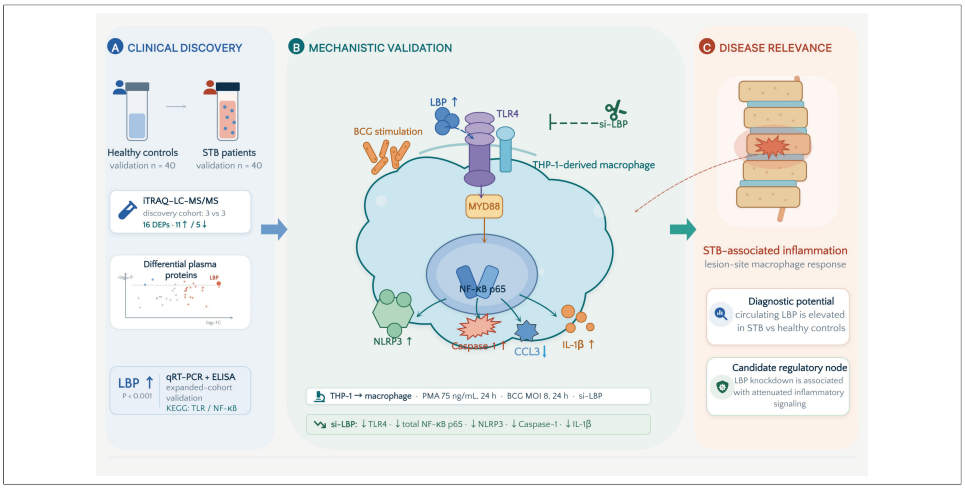

Abstract

Background: Spinal tuberculosis (STB) is a common type of extrapulmonary tuberculosis, primarily characterized by inflammatory response and vertebral bone destruction. Currently, the specific molecular regulatory mechanisms underlying the inflammatory response in STB have not been fully elucidated. Via screening differentially expressed proteins in STB samples, this study preliminarily explores the role of lipopolysaccharide-binding protein (LBP) in regulating inflammatory signal transduction.

Methods: Plasma samples from patients with STB and healthy controls were analyzed by isobaric tags for relative and absolute quantification (iTRAQ) combined with liquid chromatography-tandem mass spectrometry (LC-MS/MS). Candidate proteins were

[1]Department of Orthopedics, General Hospital of Ningxia Medical University, Yinchuan 750004, Ningxia, China.
[2]Ningxia Medical University, Yinchuan 750004, Ningxia, China.
[3]Department of Orthopedics, Zhoukou Orthopedic Hospital, Zhoukou 466000, Henan, China.
[4]Key Laboratory of Clinical Pathogenic Microorganisms, General Hospital of Ningxia Medical University, Yinchuan 750004, Ningxia, China.
[5]Department of Surgical Laboratory, Institute of Medical Sciences, General Hospital of Ningxia Medical University, Yinchuan 750004, Ningxia, China.
[6]Research Center for the Prevention and Control of Bone and Joint Tuberculosis, General Hospital of Ningxia Medical University, Yinchuan 750004, Ningxia, China.
[#,‡]These authors contributed equally to this work.

Correspondence to: Prof. Ningkui Niu, Department of Orthopedics, General Hospital of Ningxia Medical University, Yinchuan 750004, Ningxia Hui, China. E-mail: niuningkui6743242@163.com; Prof. Xu Zhang, Department of Surgical Laboratory, Institute of Medical Sciences, General Hospital of Ningxia Medical University, Yinchuan 750004, Ningxia, China. E-mail: xuzhang1012@163.com

further validated by quantitative real-time polymerase chain reaction and enzyme-linked immunosorbent assay. A Bacillus Calmette-Guérin-stimulated THP-1-derived macrophage model was used to assess the effects of LBP knockdown on Toll-like receptor 4 (TLR4)/nuclear factor kappa-B (NF-κB)-associated signaling and inflammatory mediator expression.

Results: LBP was upregulated in patients with STB. In BCG-stimulated macrophages, LBP knockdown was associated with the downregulation of TLR4/NF-κB signaling and decreased expression of inflammatory mediators, including NLRP3, Caspase-1, and interleukin-1β.

Conclusion: LBP is correlated with the inflammatory response in STB and may be related to the alteration of the TLR4/NF-κB signaling pathway. LBP may serve as a potential diagnostic biomarker and candidate regulatory molecule for STB.

INTRODUCTION

Tuberculosis (TB), caused by Mycobacterium tuberculosis (M.tb) infection, is a chronic infectious disease with widespread prevalence and a heavy disease burden. Its threat to human health has not been fully contained to date[1]. Spinal tuberculosis (STB), a common extrapulmonary form of TB, often occurs when M.tb spreads from a primary site via the bloodstream to the vertebral bodies[2]. As the condition progresses, patients may experience vertebral destruction, pathological fractures, deformities such as kyphosis, and in severe cases, neurological impairment due to spinal cord compression[3].

The lesion site in STB is usually associated with significant inflammatory cell infiltration, particularly macrophages, neutrophils, and lymphocytes. M.tb, an intracellular pathogen, primarily resides within macrophages, which play a critical role in both innate immune responses and pathogen control[4]. Macrophages, as a key component of the innate immune system, are involved in pathogen detection, immune surveillance, inflammation regulation, and microbial elimination[5]. Upon infection, these cells accumulate at the infection site, become activated, and undergo metabolic reprogramming, switching from oxidative phosphorylation to glycolysis, which further influences their polarization and the production of inflammatory mediators[6]. While macrophages limit M.tb replication, they also exacerbate tissue damage by releasing pro-inflammatory cytokines[7]. Previous research has shown that M.tb can survive in host macrophages and induce granuloma formation. Inside granulomas, the bacteria may continue to replicate, leading to caseous necrosis, liquefaction, and cavitation, thus promoting disease progression[8]. Granulomas serve as both a defense mechanism against pathogen spread and the foundation for chronic inflammation in TB.

Lipopolysaccharide-binding protein (LBP) is a soluble molecule that recognizes microbial patterns and is elevated in various infectious and inflammatory conditions[9]. LBP contributes to inflammatory responses by enhancing the release of chemokines and pro-inflammatory mediators and by modulating innate immune signaling[10]. Toll-like receptors (TLRs) are essential for detecting pathogen-associated molecular patterns and initiating innate immunity, and dysregulation of TLR signaling is associated with several autoimmune and chronic inflammatory diseases[11]. Nuclear factor-κB (NF-κB), a key regulator in the inflammatory pathway, is a major target downstream of TLRs[12]. When activated, TLRs recruit adaptor proteins such as IRAK, leading to NF-κB activation and translocation[13]. Moreover, evidence suggests that LBP amplifies TLR-related signaling and enhances the host's immune response[14]. Given the importance of macrophages in STB pathogenesis, LBP may be implicated in the regulation of inflammatory pathways and could serve as a potential biomarker and therapeutic target for STB. However, the role of LBP in macrophage responses during mycobacterial infection remains poorly understood.

This study investigates LBP expression and its role in STB using clinical samples and an *in vitro* macrophage model. Proteomics was employed to identify differentially expressed proteins in STB patients, followed by further exploration of the relationship between LBP and TLR-related inflammatory signaling using a Bacillus Calmette-Guérin (BCG)-stimulated macrophage model. Our goal is to provide insights into the molecular mechanisms underlying STB inflammation and identify potential immunoregulatory targets for therapy.

MATERIALS AND METHODS

Clinical samples

The study participants were recruited from the Department of Orthopedics at Ningxia Medical University General Hospital and included 40 patients with confirmed STB who were diagnosed between January 2021 and June 2022. The patient group consisted of 25 males and 15 females, with an age range of 37 to 73 years (mean age: 53.5 ± 4.6 years). A control group of 40 healthy volunteers was also enrolled, comprising 20 males and 20 females, aged 40 to 72 years (mean age: 51.3 ± 5.5 years). No statistically significant differences in gender distribution or age were observed between the two groups ($P > 0.05$). Patients with STB were enrolled if they had a confirmed diagnosis supported by histopathology or a combination of typical imaging features, etiological evidence and clinical manifestations, were aged 35-75 years, had not received prior anti-tuberculosis treatment, and provided written informed consent. Patients with other spinal infections, concurrent active tuberculosis at other sites, autoimmune diseases, malignancies, severe organ dysfunction, recent immunosuppressant use, or pregnancy/lactation were excluded. Healthy controls were frequency-matched for age and gender, had no history of spinal diseases or infectious disorders, showed no abnormalities in routine examinations, and provided informed consent. Individuals with a history of tuberculosis, chronic inflammatory diseases, or recent immunomodulatory drug use were excluded from the control group.

For proteomic screening, three subjects were randomly selected from the 40 participants in each group (STB and control). Subsequent validation of candidate proteins via qRT-PCR and ELISA was performed using the full cohort of 40 subjects per group. The study protocol was reviewed and approved by the Research Ethics Committee of Ningxia Medical University General Hospital, which determined that the research conformed to established ethical standards (Approval No. KYLL-2021-932). Written informed consent was obtained from all participants prior to enrollment.

iTRAQ-based proteomic analysis

Proteomic profiling was performed on both clinical plasma samples and cultured THP-1 macrophages to identify differentially expressed proteins and their associated signaling pathways. For clinical samples, peripheral plasma was collected from 3 patients with STB and 3 age- and sex-matched healthy controls; whole blood was centrifuged at 3,000 rpm for 10 min at 4 °C, and the supernatant plasma was stored at -80 °C until use. For cellular experiments, THP-1 macrophages were allocated to four groups: blank control, BCG-stimulated, LBP-knockdown control (LBP knockdown without BCG treatment), and BCG-stimulated + LBP-knockdown groups, with total cellular proteins extracted using RIPA lysis buffer supplemented with a protease inhibitor cocktail. All protein samples were quantified via the bicinchoninic acid (BCA) assay, digested into peptides with trypsin, and analyzed by liquid chromatography-tandem mass spectrometry (LC-MS/MS); specifically, plasma protein samples were labeled with isobaric tags for relative and absolute quantification (iTRAQ) before detection, while cellular protein samples were processed via the filter-aided sample preparation (FASP) method for label-free quantification. Raw mass spectrometry data were searched against the human UniProt reference database for protein identification, and differentially expressed proteins between paired groups were screened with consistent thresholds of fold change > 1.20 or < 0.83 and $P < 0.05$.

Kyoto Encyclopedia of Genes and Genomes pathway enrichment analysis

Kyoto Encyclopedia of Genes and Genomes (KEGG) pathway enrichment analysis was conducted separately on two sets of differentially expressed proteins: those identified from clinical plasma proteomic profiling, and those derived from pairwise comparisons of different THP-1 macrophage treatment groups. The clusterProfiler R package was used for enrichment analysis to delineate the signaling pathways associated with protein expression alterations under each experimental condition. The significance threshold was set at $P < 0.05$, fully consistent with the differential protein screening criteria described in Section **iTRAQ-based proteomic analysis**.

Quantitative real-time PCR (qRT-PCR)

Total RNA from blood samples was extracted using the TRIzol method (Invitrogen, USA), and cDNA was synthesized by reverse transcription of RNA using the PrimeScript RT reagent Kit (Thermo, USA). The obtained cDNA was used for qRT-PCR validation experiments on the LightCycler480II quantitative platform (Roche, USA), using β-actin as an internal reference. All 16 differentially expressed proteins identified by proteomic screening were validated at the mRNA level, and the corresponding primer sequences are listed in Table 1. The reaction system consisted of 1 μL of template cDNA, 0.4 μL each of the upstream and downstream primers, 8.2 μL of ddH2O, and 10 μL of SYBR MIX, with a total volume of 20 μL. PCR conditions were as follows: 95 °C for 3 min; 95 °C for 5 s; 60 °C for 30 s, for a total of 40 cycles. The obtained data were analyzed using the 2-ΔΔCt method to calculate the relative gene expression levels.

Enzyme-linked immunosorbent assay

Peripheral whole blood (3-5 mL) was collected from each subject, and centrifuged at 3,000 rpm for 10 min at 4 °C within 1 h after collection. The plasma supernatant was harvested and stored at -80 °C until use. After all samples were collected, target protein levels were measured using commercial enzyme-linked immunosorbent assay (ELISA) kits (Beijing Xinbosheng Biotechnology Co., Ltd.) following the manufacturer's instructions.

THP-1 cell culture and differentiation induction

The human monocytic cell line THP-1 was purchased from Wuhan Zishan Biotechnology Co., Ltd. (Wuhan, Hubei, China). Cells were routinely maintained in complete RPMI 1640 medium (Cat. No. 11875093, Gibco, USA) supplemented with 10% (v/v) heat-inactivated fetal bovine serum (FBS, Cat. No. 10099141C, Gibco, USA). All cultures were incubated in a humidified atmosphere with 5% CO_2 at 37 °C. THP-1 cells were passaged every 2-3 days at a split ratio of 1:3 to 1:4 when reaching 80%-90% confluence. Only cells within passage 5 to passage 20 were used for all formal experiments to guarantee stable cellular phenotypes and experimental reproducibility.

Cell line authentication was performed via short tandem repeat (STR) profiling. The STR genotype of the THP-1 cell line was verified by the supplier (Wuhan Zishan Biotechnology Co., Ltd., China) prior to delivery. The genotyping results were fully consistent with the standard THP-1 profile in the ATCC cell bank, and no cross-contamination with other human cell lines was detected. Mycoplasma contamination was routinely screened for all cell batches using a PCR-based mycoplasma detection kit, and all cells applied in this study were confirmed to be mycoplasma-free.

For macrophage differentiation, THP-1 cells in the logarithmic growth phase were counted using an automated cell counter and seeded into 6-well plates at a density of 5×10^6 cells per well, with 2.5 mL of complete culture medium added to each well. To optimize the differentiation condition, cells were treated with a gradient of phorbol 12-myristate 13-acetate (PMA, MCE, Cat. No. HY-18739) concentrations, and cell adherence status was evaluated at serial time points (0, 6, 12, 18, 24, 30, 36, and 48 h). A PMA concentration

Table 1. Real-time fluorescence quantitative PCR primers

Gene	Primer	Sequence (5′ → 3′)	Product
LBP	Forward	CTGGCATTGCTGCTTACGTC	164
	Reverse	CTCAAGTCCCCGGTGAAGTC	
S100A8/A9	Forward	TGTCTTTCAGAAGACCTGGTTC	140
	Reverse	ACGGCATGGAAATTCCCCTTT	
IGLV4-60	Forward	GCTGACTCAATCATCCTCTGC	171
	Reverse	CTCCCCTTGTTGTAGCTTCCA	
SAA2	Forward	TGGCTGGAAAGATGGAGACAA	115
	Reverse	AAAGCTCTCTCTTGCATCACTG	
LRG2	Forward	TTGGCAGCATCAAGGAAGC	226
	Reverse	CAGATGGACAGTGTCGGCA	
PRG4	Forward	CAGAGGTCTCTACTCCAACTACC	199
	Reverse	AGTCATTTCAGGTTTAGTCGCTG	
CFI	Forward	GGTGAGGTGGACTGCATTACA	191
	Reverse	CCTCCCACAATTCGTTTCCTTC	
SERPINA1	Forward	GGAGGCTCAGATCCATGAAGG	187
	Reverse	GGTGTCCCCGAAGTTGACAG	
CTSD	Forward	TGCTCAAGAACTACATGGACGC	117
	Reverse	CGAAGACGACTGTGAAGCACT	
CP	Forward	GGGCCATCTACCCTGATAACA	88
	Reverse	TTAAAGGTCCGATGAGTCCTGA	
VCL	Forward	CTCGTCCGGGTTGGAAAAGAG	142
	Reverse	AGTAAGGGTCTGACTGAAGCAT	
IGHV3-64D	Forward	GGACGACGTCTGTGTAGCACT	83
	Reverse	GGGCTATCTTCCGTGATCACA	
IGKV2D-29	Forward	CCGAGGTCTCATCTCGATCTTCC	129
	Reverse	AGTCATATCAGGGTTAGTCACTG	
IGKV6D-41	Forward	GCAGGACCAGATTCATCATGG	214
	Reverse	GGTCTCGTCGATGTAGACAG	
IGHV1-45	Forward	GCGGAATCGATCATTCTGTGC	96
	Reverse	CTCCTCTTGTCGTAGCATCCA	
β-actin	Forward	GAAAATCTGGCACCACAAAT	45
	Reverse	GATAGCACAGCCTGGATAGCAA	

LBP: Lipopolysaccharide-binding protein; S100-A8/A9: SAA2: serum amyloid A2; LRG2: leucine-rich alpha-2-glycoprotein 2; PRG4: proteoglycan 4; CFI: complement factor I; SERPINA1: serpin family A member 1; CTSD: cathepsin D; CP: ceruloplasmin; VCL: vinculin.

of 75 ng/mL and an induction period of 24 h were determined as optimal to differentiate THP-1 monocytes into adherent macrophage-like cells.

For BCG infection optimization, diluted BCG suspension was added to differentiated macrophages at multiplicities of infection (MOIs) of 0, 2, 4, 8, 12, 16, 20, and 24. Cell morphology, viability, and differentiation status were assessed to screen the optimal infection dose. Subsequently, time-gradient experiments (0, 6, 12, 18, 24, 30, 36, and 48 h) were performed at the optimized MOI to characterize dynamic cellular responses and determine the optimal infection duration. All incubations were conducted under the standard culture conditions described above.

Cell transfection

Small interfering RNA (siRNA) sequences targeting LBP were designed by Shanghai Gima Pharmaceutical Biotechnology Co., Ltd. A 4 OD siRNA was synthesized for use in cell transfection experiments. Under optimized conditions of concentration and incubation time, 10 μL of siRNA was mixed with 15 μL of Zeta transfection reagent in a sterile centrifuge tube, gently vortexed, and incubated at room temperature in a laminar flow hood for 20 min to allow formation of siRNA-lipid complexes. The resulting complex solution was then added dropwise to each well of a 6-well plate, with 25 μL applied per well. The plate was gently shaken to ensure uniform distribution of the transfection mixture. Cells were subsequently incubated in a standard cell culture incubator (37 °C, 5% CO_2) for 24 h, after which the culture medium was replaced. The cells were then further incubated for an additional 24 hours before proceeding to downstream assays.

Western blotting (WB)

Total cellular proteins were extracted using ice-cold RIPA lysis buffer supplemented with a protease inhibitor cocktail and a phosphatase inhibitor cocktail (Servicebio, China). After lysis on ice for 30 min with intermittent vortexing, the lysates were centrifuged at 12,000 ×*g* for 15 min at 4 °C to collect the supernatant containing total cellular proteins. Protein concentration was determined using a BCA protein assay kit (Servicebio, China).

For each sample, 30 μg of total protein was loaded and separated by 10% SDS-polyacrylamide gel electrophoresis (SDS-PAGE), and then electrotransferred onto polyvinylidene fluoride (PVDF) membranes. The membranes were blocked with 5% (w/v) skim milk powder dissolved in Tris-buffered saline with Tween-20 (TBST) for 1 h at room temperature, and then incubated with primary antibodies overnight at 4 °C. The primary antibodies used were as follows: LBP, TLR2 and TLR4 (Servicebio, China, 1:1,000); TLR9, NF-κB p65, myeloid differentiation primary response 88 (MyD88), NLR family pyrin domain containing 3 (NLRP3), Caspase-1, C-C motif chemokine ligand (CCL3), and IL-1β (Affinity, China, 1:1,000); glyceraldehyde-3-phosphate dehydrogenase (GAPDH) (Affinity, China, 1:5,000).

After five washes with TBST, the membranes were incubated with horseradish peroxidase (HRP)-conjugated secondary antibodies (Affinity, China, 1:10,000) for 1 h at room temperature. After another five washes with TBST, an enhanced chemiluminescence (ECL) reagent was added for band visualization. Finally, ImageJ software was used to quantify the grayscale values of the target bands, and relative protein expression levels were normalized to the internal reference GAPDH for comparative analysis.

Statistical analysis

All statistical analyses were performed using SPSS 26.0 software. Quantitative data are presented as mean ± standard deviation (mean ± SD). Biological replicates refer to independent experiments performed on biologically distinct samples. All sample sizes (denoted as n) in this study represent the number of biological replicates. Technical replicates refer to repeated measurements of the same biological sample. The average value of technical replicates was calculated as the final value for each corresponding biological replicate, and technical replicates were not included in the statistical sample size.

Prior to all parametric analyses, the Shapiro-Wilk test was used to verify the normality of data distribution, and Levene's test was used to assess the homogeneity of variances across groups. All datasets in this study conformed to the assumptions of normal distribution and equal variance; thus, parametric statistical methods were adopted. For two-group comparisons (including the proteomic screening with 3 samples per group, as well as qRT-PCR and ELISA validation with 40 clinical samples per group), differences between the STB group and healthy control group were analyzed by two-tailed unpaired Student's *t*-test. For multi-group comparisons (including the time-gradient and concentration-gradient optimization of BCG infection, and

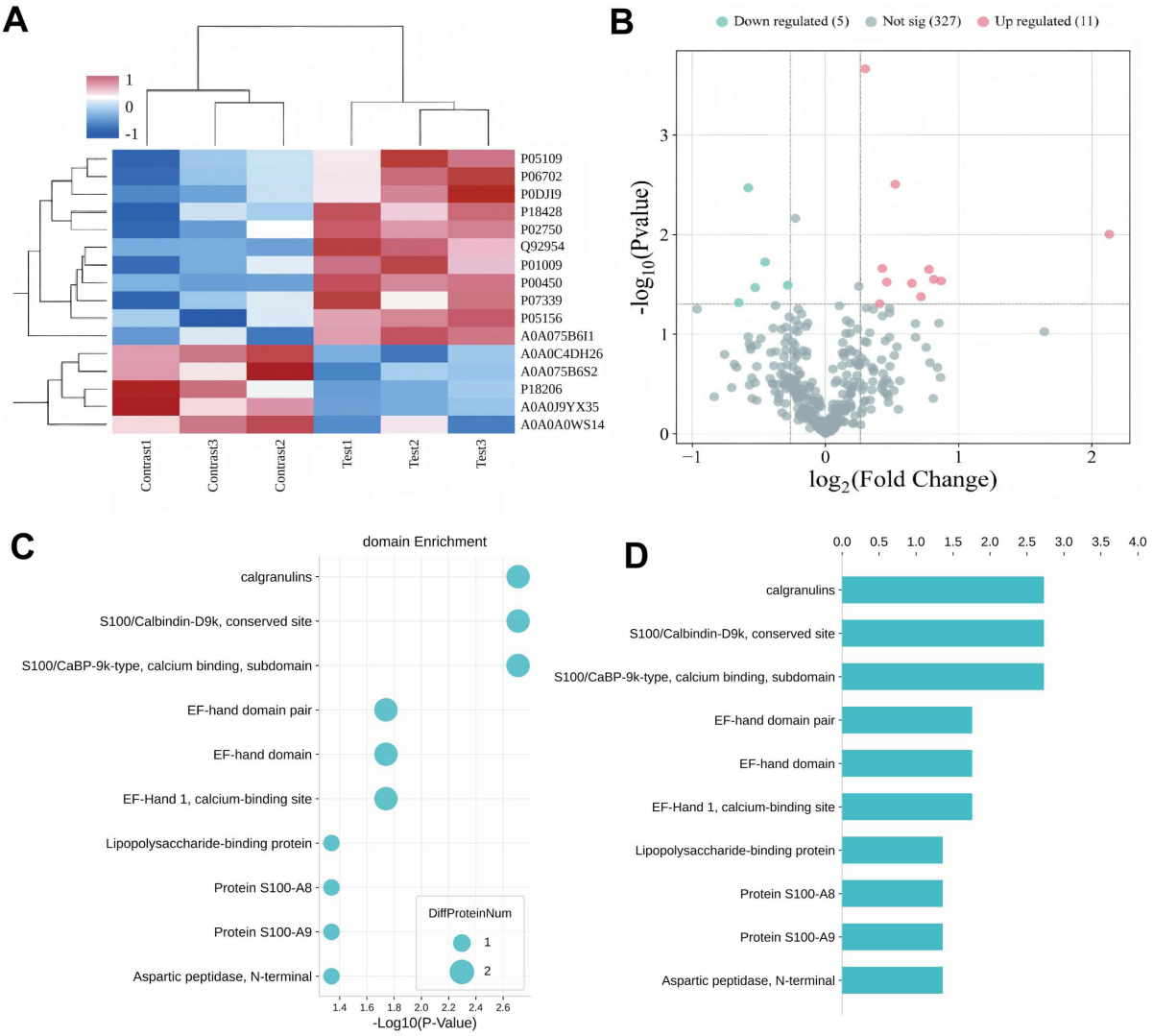

Figure 1. Differential protein screening in peripheral blood from patients with STB. (A) Differential Protein Clustering Analysis; (B) Differential Protein Volcano Distribution Plot; (C) Differential Protein Domain Bubble Chart; (D) Differential Protein Domain Bar Chart. *n* = 3 subjects per group. STB: Spinal tuberculosis.

the four-group cell intervention experiment), overall differences among groups were analyzed by one-way analysis of variance (one-way ANOVA), and Tukey's post-hoc test was applied for pairwise multiple comparison correction. A P-value < 0.05 was considered statistically significant.

RESULTS

Identification of differentially expressed proteins in plasma samples from patients with STB

Using iTRAQ combined with LC-MS/MS, the plasma protein expression profiles of patients with STB and healthy controls were compared. Differentially expressed proteins (DEPs) were screened using the criteria of fold change (FC) > 1.20 or < 0.83 and P < 0.05. A total of 16 DEPs were identified between the two groups, including 11 upregulated proteins and 5 downregulated proteins in the STB group [Figure 1A and B]. The overall distribution of DEPs was visualized by volcano plot analysis, and hierarchical clustering analysis further demonstrated distinct protein expression patterns between the STB group and the healthy control group.

Table 2. qRT-PCR validation of differential gene expression in peripheral blood samples from patients with STB and healthy controls

Gene name	Normal group measurements	Measured values in patients with STB	*P* value
LBP	0.97 ± 0.36	1.63 ± 0.31	< 0.001
S100A8/A9	0.87 ± 0.35	1.46 ± 0.26	< 0.001
IGLV4-60	0.79 ± 0.26	0.86 ± 0.38	0.339
SAA2	1.35 ± 0.25	1.25 ± 0.82	0.463
LRG2	0.76 ± 0.31	0.86 ± 0.23	0.105
PRG4	0.81 ± 0.31	0.89 ± 0.27	0.222
CFI	0.83 ± 0.52	0.77 ± 0.46	0.586
SERPINA1	0.75 ± 0.31	0.89 ± 0.62	0.205
CTSD	0.76 ± 0.46	0.67 ± 0.54	0.425
CP	0.84 ± 0.57	0.74 ± 0.51	0.411
VCL	0.61 ± 0.39	0.73 ± 0.31	0.132
IGHV3-64D	0.89 ± 0.43	0.75 ± 0.47	0.168
IGKV2D-29	0.85 ± 0.39	0.76 ± 0.48	0.360
IGKV6D-41	0.76 ± 0.43	0.89 ± 0.53	0.232
IGHV1-45	0.75 ± 0.34	0.87 ± 0.59	0.269

qRT-PCR: quantitative real-time PCR; STB: spinal tuberculosis; LBP: lipopolysaccharide-binding protein; S100-A8/A9: SAA2: serum amyloid A2; LRG2: leucine-rich alpha-2-glycoprotein 2; PRG4: proteoglycan 4; CFI: complement factor I; SERPINA1: serpin family A member 1; CTSD: cathepsin D; CP: ceruloplasmin; VCL: vinculin.

To comprehensively verify the differential expression of all screened proteins, all 16 DEPs were subjected to qRT-PCR validation at the mRNA level. Based on the magnitude of differential expression, statistical significance, and potential biological relevance to STB pathogenesis, 10 core candidate proteins closely associated with innate immunity, inflammatory regulation and tissue remodeling were further selected for protein-level validation by ELISA and subsequent mechanistic exploration. These core candidate proteins included LBP, S100 calcium-binding protein A8/A9 (S100A8/A9), serum amyloid A2 (SAA2), leucine-rich alpha-2-glycoprotein 2 (LRG2), proteoglycan 4 (PRG4), complement factor I (CFI), serpin family A member 1 (SERPINA1), cathepsin D (CTSD), ceruloplasmin (CP), and vinculin (VCL) [Figure 1C and D].

Validation of differential gene expression by qRT-PCR

qRT-PCR of peripheral blood gene expression in patients with STB and healthy controls revealed that the LBP and *S100A8/A9* genes were significantly overexpressed ($P < 0.05$). In addition, the genes *SAA2*, *LRG2*, *PRG4*, *CFI*, *SERPINA1*, *CTSD*, *CP*, *VCL*, *IGLV4-60*, *IGHV3-64D*, *IGKV2D-29*, *IGKV6D-41*, and *IGHV1-45* showed either upregulation or downregulation in peripheral blood samples from STB patients; however, these changes did not reach statistical significance ($P > 0.05$, $n = 40$ subjects per group) [Table 2].

The expression levels of differentially expressed proteins in peripheral blood were verified by ELISA

The proteins were quantified in patients with STB using commercial ELISA kits. The results demonstrated that plasma levels of LBP and S100-A8/S100-A9 in STB patients were significantly elevated compared to controls, and their protein expression showed a positive correlation with corresponding gene expression at the transcriptional level. In contrast, no significant differences in protein levels were observed for SAA2, LRG2, PRG4, CFI, SERPINA1, CTSD, CP, or VCL between STB patients and healthy controls, and the expression of these proteins did not correlate with their respective mRNA levels. These discrepancies may reflect post-transcriptional regulation, secretion dynamics, protein stability, or differences between cellular transcription and circulating protein abundance [Figure 2].

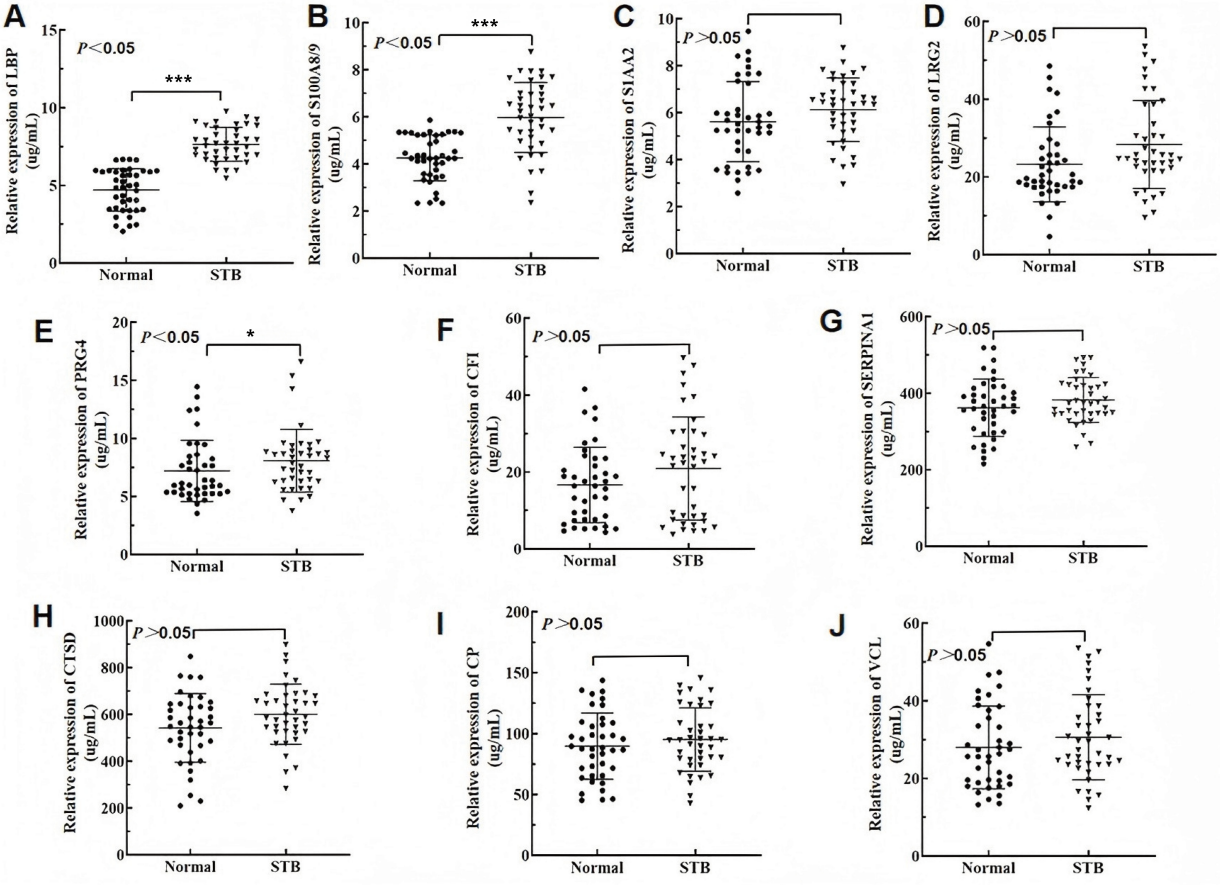

Figure 2. ELISA detection of differentially expressed proteins in peripheral blood from healthy individuals and patients with STB. (A-J) The expression differences of different proteins in STB and the normal control group. ns ($P > 0.05$), * ($P < 0.05$), *** ($P < 0.001$), $n = 40$ subjects per group. STB: Spinal tuberculosis; LBP:lipopolysaccharide-binding protein; S100A8/A9: S100 calcium-binding protein A8/A9; SAA2: serum amyloid A2; LRG2: leucine-rich alpha-2-glycoprotein 2; PRG4: proteoglycan 4; CFI: complement factor I; SERPINA1: serpin family A member 1; CTSD: cathepsin D; CP: ceruloplasmin; VCL: vinculin; ELISA: enzyme-linked immunosorbent assay.

KEGG enrichment analysis associated with STB

KEGG pathway enrichment analysis identified several significantly enriched signaling pathways related to the differentially expressed proteins [Table 3]. Notably, LBP was annotated to the TLR and NF-κB signaling pathways, which were identified as significantly enriched pathways among the differentially expressed proteins. These findings suggest that the identified differentially expressed proteins and their associated signaling pathways may play critical roles in the pathogenesis of STB.

KEGG enrichment analysis of differential proteins under different treatment conditions

To delineate the functional signaling pathways modulated by BCG stimulation and LBP knockdown in macrophages, KEGG pathway enrichment analysis was performed on differentially expressed proteins derived from each of the four THP-1 macrophage treatment groups, and the corresponding enrichment profiles are shown in Figure 3A-D. The results demonstrated that the differentially expressed proteins under different intervention conditions were predominantly associated with multiple innate immune and inflammatory-related pathways, including the Toll-like receptor signaling pathway, TNF signaling pathway, and IL-17 signaling pathway.

Notably, the Toll-like receptor signaling pathway and its downstream NF-κB signaling cascade were consistently identified as core enriched pathways, which were fully consistent with the pathway annotation of LBP, the key differential molecule screened from the plasma proteomics of STB patients. This concordance

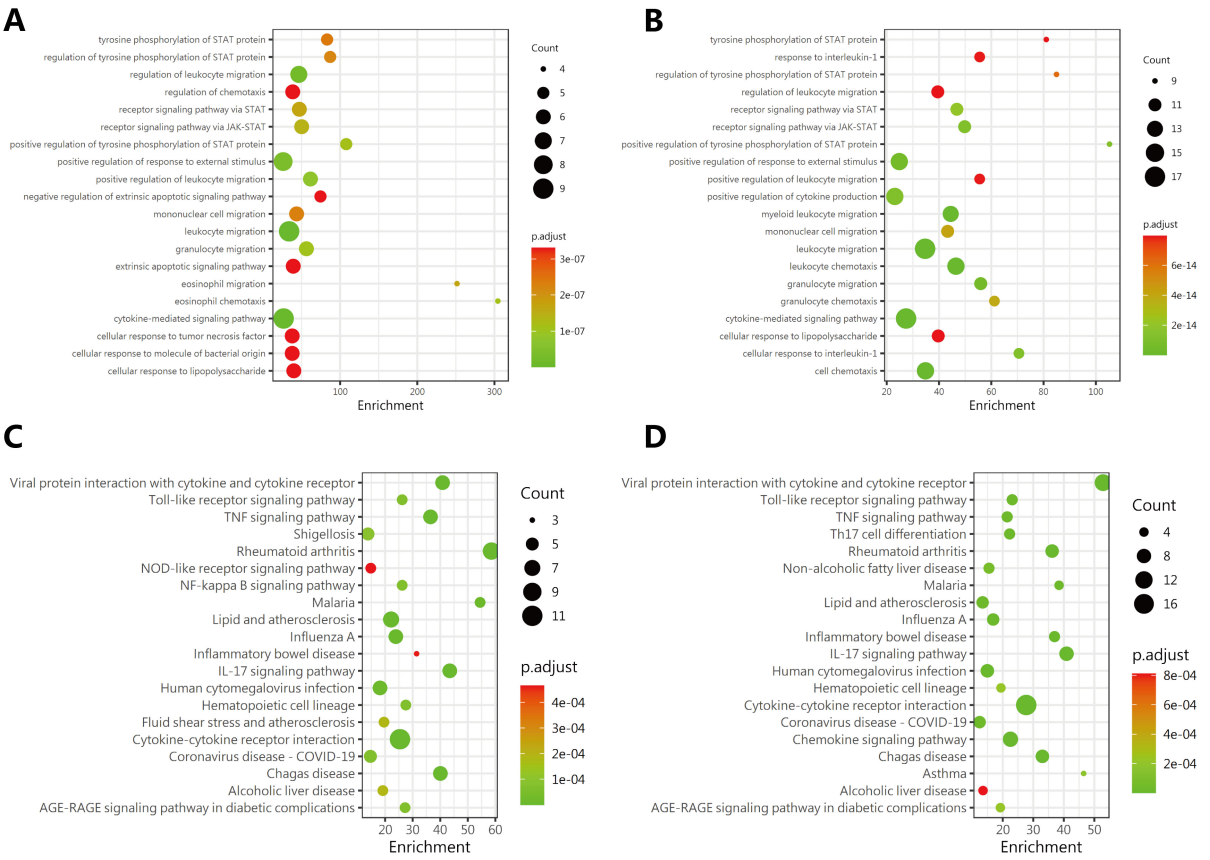

Figure 3. KEGG pathway enrichment analysis of differentially expressed proteins in THP-1-derived macrophages under different treatment conditions. (A) Differential protein-related signaling pathways in the blank control group; (B) Differential protein-related signaling pathways in the BCG group; (C) Differential protein-related signaling pathways in the LBP knockdown + control group; (D) Differential protein-related signaling pathways in the BCG + LBP knockdown group. IL: Interleukin; BCG: Bacillus Calmette-Guérin; LBP: lipopolysaccharide-binding protein; TNF: tumor necrosis factor; NOD: nucleotide-binding oligomerization domain; KEGG: Kyoto Encyclopedia of Genes and Genomes.

Table 3. KEGG signaling pathway analysis results

Protein ID	Protein name	*P*-Value	Pathway
P18428	LBP	0.001	NF-κB Toll-like receptor
P05109	protein S100-A8	0.015	IL-17
P06702	protein S100-A9	0.044	IL-17
P05156	CFI	0.023	NF-κB
P01009	alpha-1-antitrypsin	0.015	Complement and coagulation cascades
P00450	CP	0.035	Porphyrin and chlorophyll metabolism
P18206	VCL	0.001	Regulation of actin cytoskeleton
A0A0J9YX35	immunoglobulin heavy chain	0.026	PI3K-Akt
A0A0A0MS14	immunoglobulin heavy chain	0.009	Calcium

KEGG: Kyoto Encyclopedia of Genes and Genomes; LBP: lipopolysaccharide-binding protein; CFI: complement factor I; CP: ceruloplasmin; VCL: vinculin; IL: interleukin.

between clinical sample profiling and *in vitro* cellular experiments further suggests that these differential proteins and their related signaling pathways may participate in the inflammatory response and pathological progression of STB.

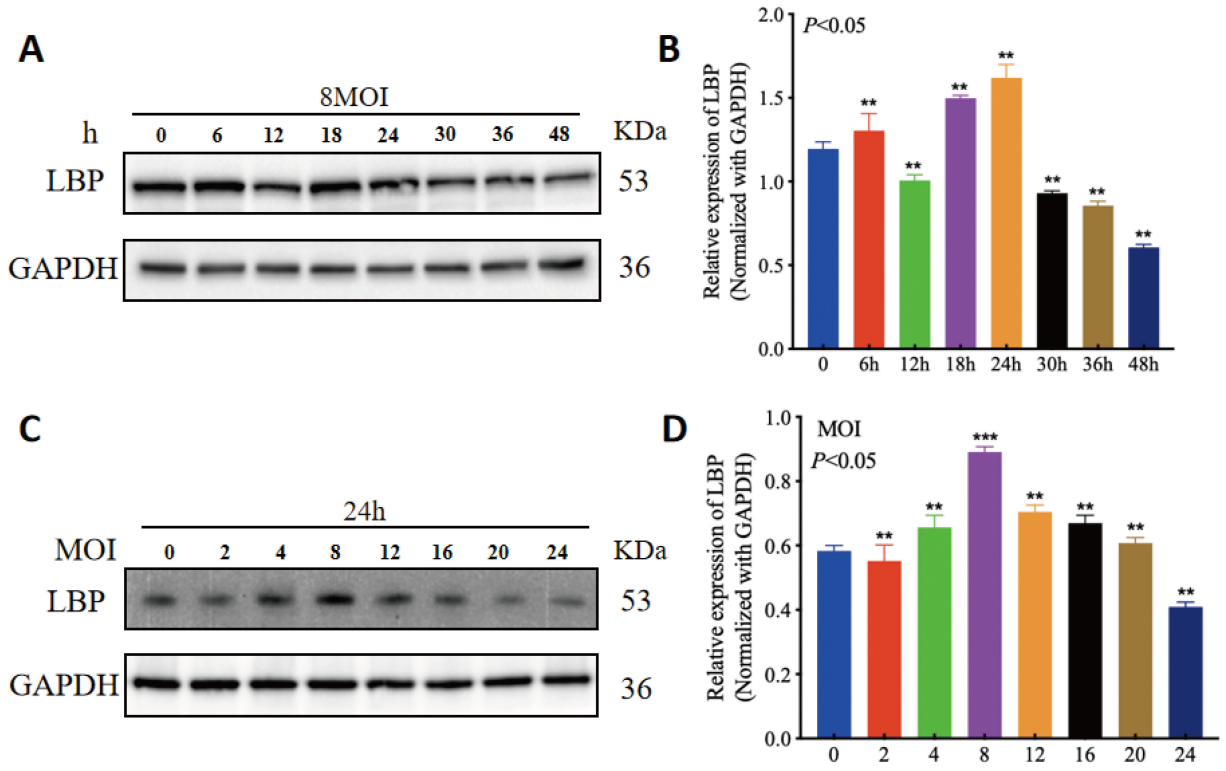

Figure 4. Determination of the optimal time and concentration for BCG infection in THP-1 human macrophages. (A-D) The optimal infection time and MOI were further validated by WB analysis, with an MOI of 8 and an infection time of 24 h identified as optimal. All data are presented as mean ± standard deviation. ** ($P < 0.01$), *** ($P < 0.001$), $n = 3$. LBP: Lipopolysaccharide-binding protein; GAPDH: glyceraldehyde-3-phosphate dehydrogenase; BCG: Bacillus Calmette-Guérin; THP-1: WB: western blotting; MOI: multiplicity of infection.

Validation of the optimal and time-dependent concentration of BCG for infection of THP-1 macrophages

Under the conditions of inducing THP-1 monocytes into macrophages, concentration and time gradients were systematically evaluated. Based on prior studies, differentiation was assessed at time points of 0, 6, 12, 18, 24, 30, 36, and 48 hours. The MOI gradients tested were 0, 2, 4, 8, 12, 16, 20, and 24. The results demonstrated that the optimal incubation time for BCG infection was 24 h, with an optimal concentration of 8 MOI [Figure 4].

Effects of LBP knockdown on TLR expression in BCG-stimulated macrophages

To further investigate the potential association between LBP and TLR-related inflammatory signaling, the expression levels of TLR2, TLR4, and TLR9 were examined in THP-1-derived macrophages under different treatment conditions. Compared with the control group, the expression of LBP was increased in BCG-stimulated macrophages. Under the same conditions, TLR4 expression was also elevated, whereas no obvious changes were observed in TLR2 or TLR9 expression.

Following siRNA-mediated knockdown of LBP, the protein expression levels of LBP and TLR4 were reduced in BCG-stimulated macrophages compared with those in the BCG group. In contrast, the expression levels of TLR2 and TLR9 showed no marked changes after LBP knockdown. These findings suggest that LBP may be associated with TLR4-related signaling changes in BCG-stimulated macrophages [Figure 5].

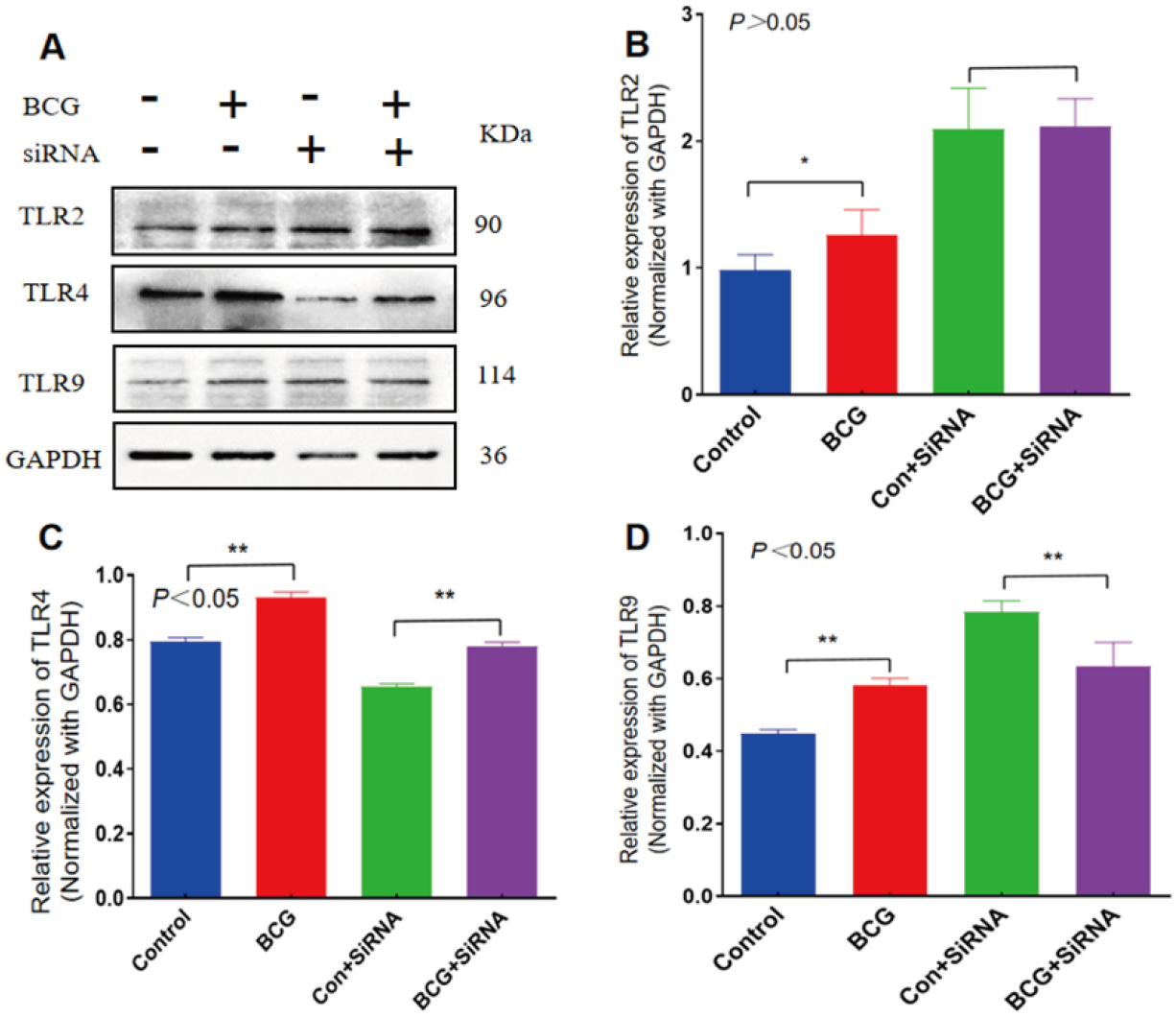

Figure 5. Results regarding the effects of BCG infection on different TLR receptors are as follows. (A-D) The protein expression levels of TLR2, TLR4, and TLR9 under BCG infection and Si-LBP interference conditions are shown. All data are presented as mean ± standard deviation. ns ($P > 0.05$), * ($P < 0.05$), ** ($P < 0.01$), $n = 3$. BCG: Bacillus Calmette-Guérin; TLR: Toll-like receptor; GAPDH: glyceraldehyde-3-phosphate dehydrogenase; LBP: lipopolysaccharide-binding protein; SiRNA: small interfering RNA.

Effects of LBP knockdown on NF-κB-associated signaling in BCG-stimulated macrophages

To further assess the association between LBP and NF-κB inflammatory signaling, the total protein expression level of NF-κB p65 was examined in THP-1-derived macrophages under different treatment conditions. Compared with the control group, BCG stimulation increased the total protein levels of LBP, TLR4, and NF-κB p65. Following siRNA-mediated knockdown of LBP, the total NF-κB p65 protein level was reduced in BCG-stimulated macrophages compared with the BCG-only group.

These findings suggest that LBP knockdown is associated with attenuated NF-κB-related signaling changes in BCG-stimulated macrophages, indicating that LBP may be involved in the regulation of inflammatory signaling under mycobacterial infection conditions [Figure 6].

Effects of LBP knockdown on inflammatory mediator expression in BCG-stimulated macrophages

To further evaluate the effects of LBP on inflammatory mediator expression, the protein levels of NLRP3, MyD88, Caspase-1, interleukin-1β (IL-1β), and CCL3 were examined in THP-1-derived macrophages under different treatment conditions. Compared with the control group, BCG stimulation increased the expression

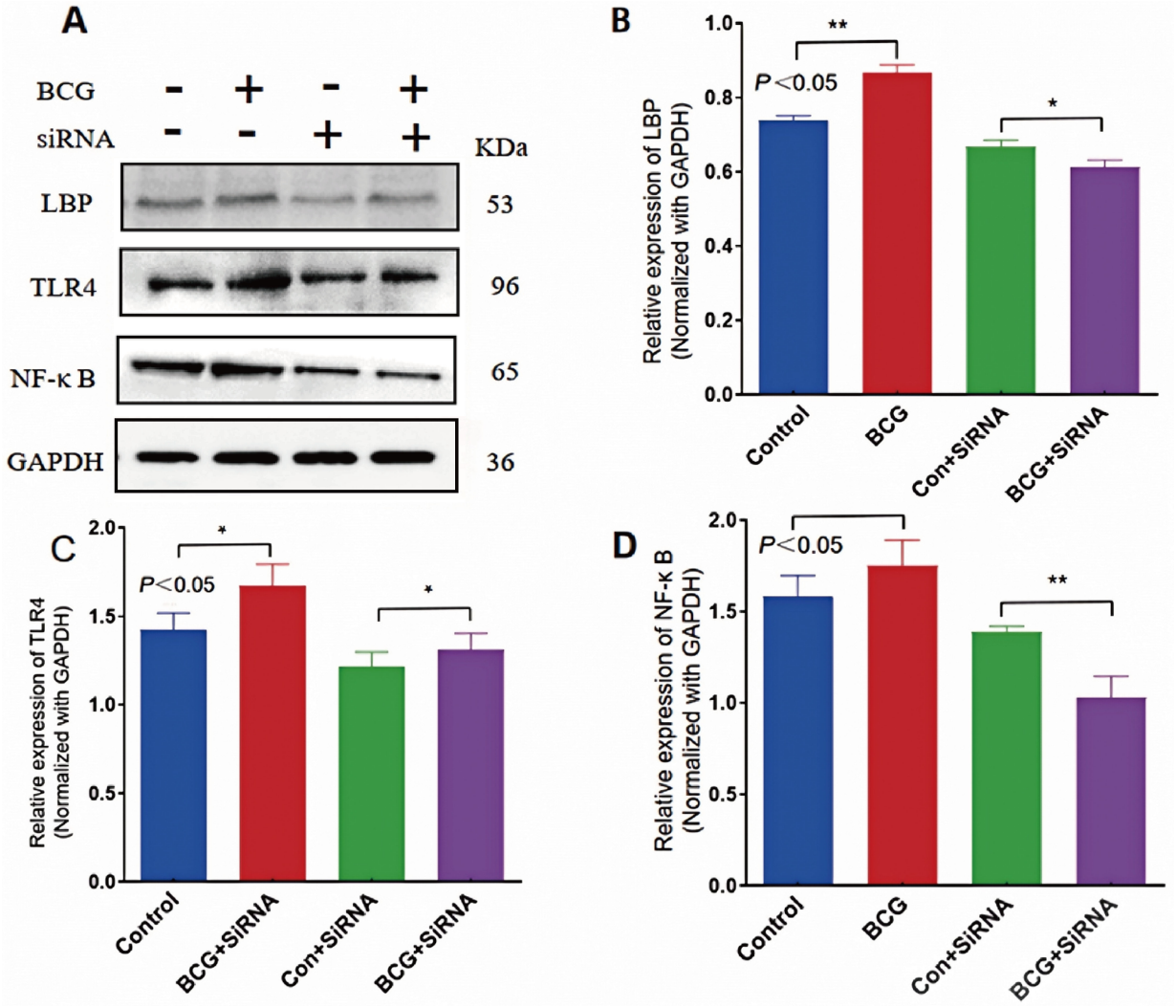

Figure 6. Effects of LBP knockdown on TLR4/NF-κB-associated protein expression in BCG-stimulated macrophages. (A-D) The protein expression levels of LBP, TLR4, and total NF-κB p65 under BCG infection and Si-LBP interference conditions are presented. All data are presented as mean ± standard deviation. ns ($P > 0.05$), * ($P < 0.05$), ** ($P < 0.01$), $n = 3$. BCG: Bacillus Calmette-Guérin; SiRNA: small interfering RNA; LBP: lipopolysaccharide-binding protein; TLR: Toll-like receptor; NF-κB: nuclear factor kappa-B; GAPDH: glyceraldehyde-3-phosphate dehydrogenase.

of NLRP3, Caspase-1, and IL-1β [Figure 7]. After siRNA-mediated knockdown of LBP, the expression levels of these inflammatory mediators were reduced in BCG-stimulated macrophages compared with those in the BCG group. For the signaling adaptor protein MyD88, no statistically significant difference in total protein expression was observed between the BCG-stimulated group and the blank control group. Compared with the BCG+siRNA group, the Con+siRNA group showed an upregulated baseline level of MyD88 protein.

In addition, CCL3 expression was altered under BCG stimulation and following LBP knockdown. Taken together, these findings suggest that LBP may be involved in the regulation of inflammatory mediator expression in BCG-stimulated macrophages [Figure 8].

DISCUSSION

STB is the most prevalent form of extrapulmonary skeletal tuberculosis, and progressive inflammatory damage is the core driver of vertebral bone destruction and disease deterioration[15]. However, the key regulatory molecules and specific signaling pathways underlying STB-associated inflammatory dysregulation

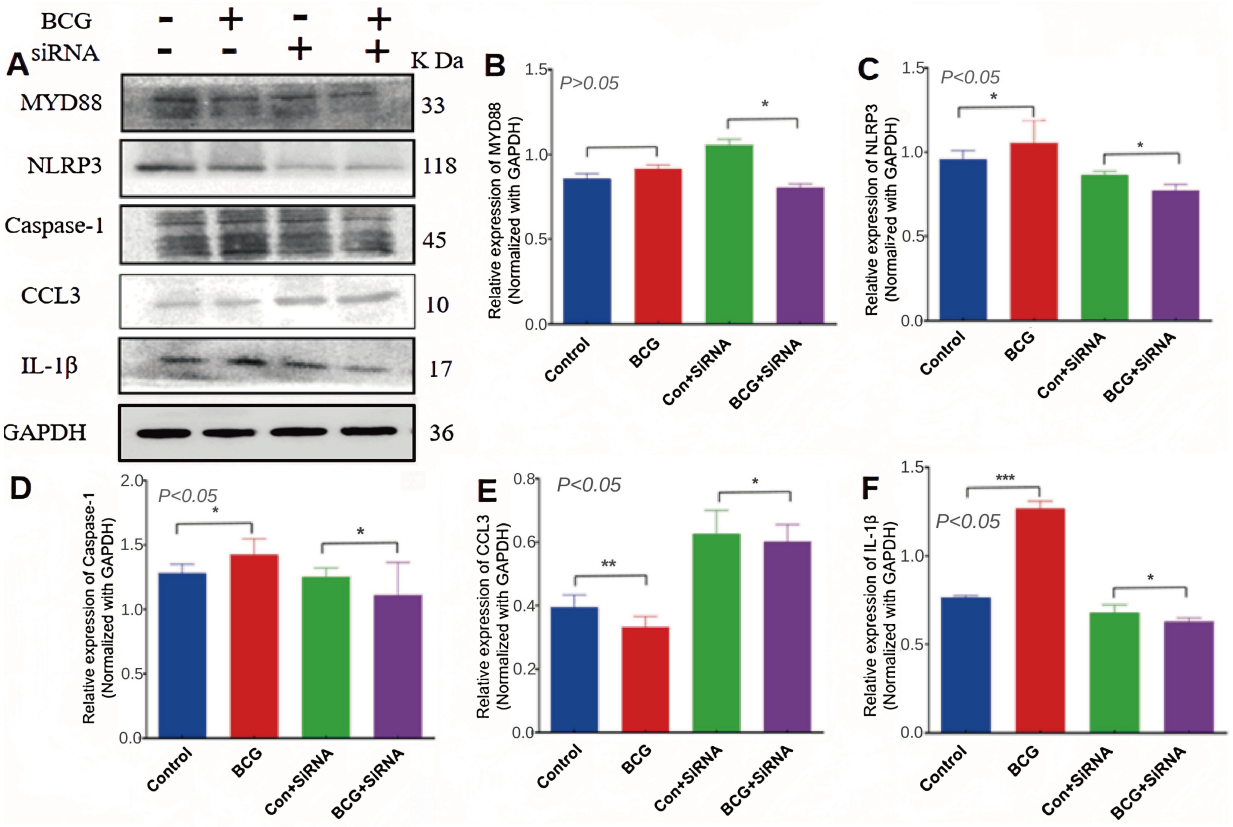

Figure 7. Under BCG infection conditions, the impact of the NF-κB signaling pathway on the expression of inflammatory cytokine proteins. (A-F) The protein expression levels of MyD88, NLRP3, Caspase-1, CCL3, and IL-1β under BCG infection and Si-LBP interference conditions are presented. All data are presented as mean ± standard deviation. ns ($P > 0.05$), * ($P < 0.05$), *** ($P < 0.001$), $n = 3$. BCG: Bacillus Calmette-Guérin; SiRNA: small interfering RNA; MyD88: myeloid differentiation primary response 88; NLRP3: NLR family pyrin domain containing 3; CCL3: C-C motif chemokine ligand; IL-1β: interleukin-1β; GAPDH: glyceraldehyde-3-phosphate dehydrogenase; LBP: lipopolysaccharide-binding protein.

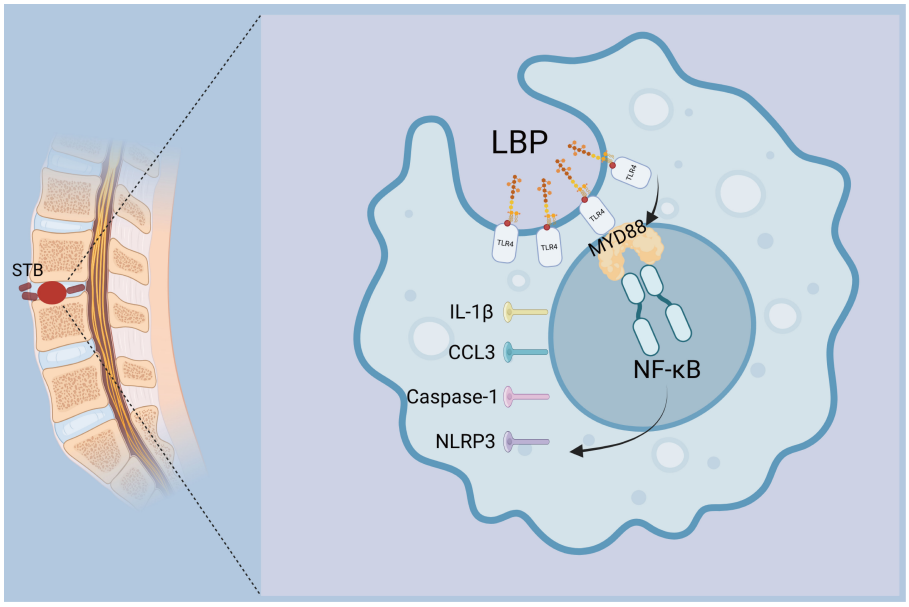

Figure 8. Schematic illustration of the putative mechanism of LBP in STB-associated inflammation. Under mycobacterial stimulation, upregulated LBP is correlated with changes in the TLR4/NF-κB signaling axis, and is associated with increased expression of downstream inflammatory mediators including NLRP3, Caspase-1, IL-1β and CCL3, which may contribute to the inflammatory progression of spinal tuberculosis. Created in BioRender. Wangjiong, W. (2026) https://BioRender.com/qnzcqqs. STB: Spinal tuberculosis; LBP: lipopolysaccharide-binding protein; IL-1β: interleukin-1β; CCL3: C-C motif chemokine ligand; NLRP3: NLR family pyrin domain containing 3; NF-κB: nuclear factor kappa-B; MyD88: myeloid differentiation primary response 88; TLR4: Toll-like receptor 4.

remain poorly defined.

In this study, we adopted a two-stage research strategy combining clinical plasma proteomics and *in vitro* cellular mechanistic validation. First, we screened differentially expressed plasma proteins between STB patients and healthy controls via iTRAQ-based quantitative proteomics, and identified LBP as a significantly upregulated candidate molecule. Subsequent expanded cohort validation confirmed consistent elevation of LBP at the plasma protein level in STB patients. In BCG-stimulated THP-1 macrophages, siRNA-mediated knockdown of LBP was associated with downregulation of TLR4/NF-κB signaling and decreased production of downstream inflammatory mediators including NLRP3, Caspase-1, and IL-1β. Collectively, these findings suggest that LBP participates in the regulation of mycobacteria-induced inflammatory responses, and may serve as a promising candidate diagnostic biomarker for STB.

LBP is a well-characterized soluble pattern recognition molecule that mediates the transfer of bacterial lipid ligands to innate immune receptor complexes[16].

Clinically, the elevated plasma LBP in STB patients is predominantly synthesized and secreted by the liver as a canonical acute-phase reactant, triggered by systemic pro-inflammatory cytokines (e.g., IL-6) during infection[17]. Circulating hepatic LBP can extravasate into vertebral lesion sites to participate in local mycobacterial antigen recognition[18]. Meanwhile, lesion-infiltrating macrophages also produce LBP locally, which amplifies inflammatory signaling in an autocrine/paracrine manner[19]. In our study, BCG stimulation significantly upregulated both LBP and TLR4 expression in THP-1 macrophages, while siRNA-mediated LBP knockdown concordantly reduced TLR4 protein levels and downstream inflammatory mediator production. These results indicate a close functional association between LBP and TLR4 signaling during mycobacterial infection.

Based on the canonical function of LBP as an extracellular lipid carrier, we postulate that the attenuated inflammatory response following LBP knockdown is primarily attributable to impaired ligand presentation to the TLR4 receptor complex. LBP binds to mycobacterial cell wall components such as lipoarabinomannan, and facilitates their recognition by the membrane CD14/TLR4 complex to initiate downstream signaling[20]. Given that BCG was administered extracellularly in our experimental system, the observed effect of LBP silencing is most likely mediated by reduced cell surface antigen presentation, rather than direct intracellular signal transduction. Nevertheless, we acknowledge that the current data cannot definitively exclude a potential intracellular regulatory role of LBP. Further experiments using intracellular targeted LBP expression or membrane-impermeable LBP inhibitors are required to clarify the exact mode of action.

Regarding the adaptor protein MyD88, we observed no significant change in total protein abundance upon BCG stimulation. This is consistent with its established function as a constitutively expressed cytoplasmic adaptor: MyD88 activation depends on its recruitment to activated membrane receptor complexes, rather than upregulation of total protein levels[10]. In addition, the slight increase in baseline MyD88 expression in the negative control siRNA group represents a well-documented non-specific effect in macrophage transfection experiments, resulting from mild innate immune activation triggered by exogenous nucleic acids and transfection reagents.

Notably, our study only assessed total NF-κB p65 protein levels, which do not directly reflect the activation status of the NF-κB pathway. Canonical NF-κB activation is defined by phosphorylation and subsequent nuclear translocation of the p65 subunit, rather than changes in total cellular protein abundance[21,22]. Therefore, our findings only demonstrate an association between LBP expression and NF-κB signaling, and do not confirm a direct regulatory effect on pathway activation. Follow-up studies will examine

phosphorylated NF-κB p65 and its subcellular localization to elucidate the precise impact of LBP on NF-κB pathway activation.

Beyond the LBP-centered TLR4/NF-κB axis, our KEGG enrichment analysis revealed multiple dysregulated pathways involved in STB pathogenesis. The IL-17 signaling pathway, driven by upregulated S100A8/A9, is strongly linked to inflammatory cascade amplification and osteoclast activation[23], which may contribute to vertebral bone destruction in STB. The complement and coagulation cascades pathway, modulated by differentially expressed SERPINA1 and CFI, reflects dysregulated innate immune defense and coagulation homeostasis during tuberculosis infection[24]. Enrichment of the actin cytoskeleton regulation pathway further suggests that aberrant cell adhesion and tissue remodeling participate in the formation of local STB lesions. Collectively, these findings delineate a complex molecular regulatory network underlying STB and provide promising directions for future mechanistic investigations.

We observed discordant expression between peripheral blood mRNA and plasma protein levels for several candidates (SAA2, LRG2, CFI, SERPINA1). This transcript-protein uncoupling, a well-documented phenomenon in clinical multi-omics research, is driven by three core biological mechanisms. First, multi-layered post-transcriptional and post-translational regulation (e.g., microRNA-mediated translational repression, alternative splicing, glycosylation, and proteolytic cleavage) decouples mRNA abundance from mature protein levels[25]. Second, circulating proteins have distinct half-lives and clearance kinetics, and secreted protein accumulation in plasma typically lags behind transcriptional changes[26], particularly in chronic infections such as STB. Third, most plasma acute-phase proteins are predominantly liver-derived, while whole-blood mRNA mainly reflects the transcriptome of circulating immune cells[27]; this tissue origin difference is a major contributor to the observed discrepancy.

Several limitations of the present work should be acknowledged.

First, the discovery-phase proteomic screening included only 3 participants per group, which is relatively small for high-dimensional omics studies and carries an inherent risk of false-positive findings. To address this limitation, we adopted a classic two-stage study design: small-sample exploratory screening followed by targeted validation in an expanded cohort. The differential expression of the core target LBP was successfully verified in the 40-patient validation cohort, which supports the reliability of our core conclusion.

Power analysis confirmed that a sample size of 40 per group provides 80% statistical power to detect moderate-to-large effect size differences at a two-sided significance level of 0.05 using unpaired Student's *t*-test, which is adequate for biomarker validation studies. However, all samples were recruited from a single medical center, which may limit the generalizability of our findings to other populations.

Second, our control group only included healthy individuals, and no patients with other spinal infectious diseases (e.g., pyogenic spondylitis, brucellar spondylitis) were enrolled. Therefore, the diagnostic specificity of LBP for STB cannot be fully evaluated in the current study.

Third, our mechanistic experiments were limited to loss-of-function assays via LBP knockdown. Gain-of-function experiments, such as LBP overexpression and functional rescue assays, were not performed, so the causal regulatory role of LBP in the TLR4/NF-κB inflammatory axis has not been fully established.

Fourth, all *in vitro* experiments were conducted using the THP-1 monocytic cell line. Immortalized cell lines differ from primary macrophages in phenotypic characteristics and inflammatory response profiles, and simplified *in vitro* models cannot fully recapitulate the complex immune microenvironment and intercellular

crosstalk of STB lesions *in vivo*. The physiological relevance of our findings requires further validation in primary macrophage models and *in vivo* STB animal models.

Future studies will expand to multi-center cohorts with disease control groups, and conduct in-depth mechanistic validation using overexpression rescue assays, primary cell models and *in vivo* animal models, to comprehensively clarify the role of LBP in STB pathogenesis.

CONCLUSIONS

In summary, LBP was upregulated in patients with STB, and LBP knockdown was associated with attenuated TLR4/NF-κB signaling and decreased expression of inflammatory mediators including NLRP3, Caspase-1, and IL-1β in a BCG-stimulated macrophage model. These findings suggest that LBP is correlated with the inflammatory response in STB and may be related to the alteration of the TLR4/NF-κB signaling pathway. LBP may serve as a potential diagnostic biomarker and candidate regulatory molecule for STB.

DECLARATIONS

Authors' contributions

Conceived the study and drafted the manuscript: Wang J, Lou C
Secured funding and critically revised the manuscript: Zhang X, Niu N
Provided technical guidance and revised the figures: Liu J, Ma H
Collected and curated the clinical data: Liu H, Shi Z
All authors reviewed and approved the final version of the manuscript.

Availability of data and materials

The datasets generated and analyzed during this study are not publicly available due to privacy and ethical restrictions, but may be made available upon reasonable request from the corresponding author, subject to appropriate data use agreements and institutional ethics approval.

AI and AI-assisted tools statement

During the preparation of this manuscript, the AI tool Doubao (version 2.0, released 2026-2-14) was used solely for language editing. The tool did not influence the study design, data collection, analysis, interpretation, or the scientific content of the work. All authors take full responsibility for the accuracy, integrity, and final content of the manuscript.

Financial support and sponsorship

This project was supported by the National Natural Science Foundation of China (No. 82260436), the Ningxia Natural Science Foundation (No. 2025AAC030752) and the Autonomous Region Key Research and Development Plan Project (No. 2026BEG02018).

Conflicts of interest

The authors declare no competing interests.

Ethics approval and consent to participate

This study was conducted in accordance with the ethical principles outlined in the Declaration of Helsinki. Ethical approval was obtained from the Ethics Committee of the General Hospital of Ningxia Medical University (Approval No. KYLL-2021-932). Written informed consent was obtained from the patient.

Consent for publication

Not applicable.

REFERENCES

1. Goletti D, Meintjes G, Andrade BB, Zumla A, Shan Lee S. Insights from the 2024 WHO global tuberculosis report - more comprehensive action, innovation, and investments required for achieving WHO end TB goals. *Int J Infect Dis.* 2025;150:107325. DOI PubMed
2. Xue D, Chen X, Shao L, et al. Risk factors for the progression from pulmonary tuberculosis to spinal tuberculosis: a logistic regression analysis. *J Orthop Surg.* 2025;20:422. DOI PubMed PMC
3. Sendrea B, Periferakis A, Periferakis A, et al. Infectious spondylodiscitis of bacterial causes in adults: epidemiology, pathophysiology, diagnostic and treatment challenges. *Microorganisms.* 2026;14:1110. DOI PubMed PMC
4. Huang L, Nazarova EV, Russell DG. *Mycobacterium tuberculosis*: bacterial fitness within the host macrophage. *Microbiol Spectr.* 2019;7:7.2.04. DOI PubMed PMC
5. Shi L, Jiang Q, Bushkin Y, Subbian S, Tyagi S. Biphasic dynamics of macrophage immunometabolism during *Mycobacterium tuberculosis* infection. *mBio.* 2019;10:e02550-18. DOI PubMed PMC
6. Prosser G, Brandenburg J, Reiling N, Barry CE, Wilkinson RJ, Wilkinson KA. The bacillary and macrophage response to hypoxia in tuberculosis and the consequences for T cell antigen recognition. *Microbes Infect.* 2017;19:177-92. DOI PubMed PMC
7. Ravesloot-Chávez MM, Van Dis E, Stanley SA. The innate immune response to *Mycobacterium tuberculosis* infection. *Annu Rev Immunol.* 2021;39:611-37. DOI PubMed
8. He Y, Xie X, He S, Li S, Zhou H, Wei S. Immunotherapy for tuberculosis: current landscape, mechanistic insights, and translational perspectives. *Front. Immunol.* 2026;17:1859046. DOI PubMed PMC
9. Lou C, Liu J, Ren Z, et al. Analysis of the value of serum biomarker LBP in the diagnosis of spinal tuberculosis. *Infect Drug Resist.* 2022;15:4915-26. DOI PubMed PMC
10. Luo R, Yao Y, Chen Z, Sun X. An examination of the LPS-TLR4 immune response through the analysis of molecular structures and protein-protein interactions. *Cell Commun Signal.* 2025;23:142. DOI PubMed PMC
11. Mukherjee S, Huda S, Sinha Babu SP. Toll-like receptor polymorphism in host immune response to infectious diseases: a review. *Scand J Immunol.* 2019;90:e12771. DOI PubMed
12. Elhadedy N, Alotaibi A, Mcgarry L, Carmody RJ. Toll-like receptor responses are shaped by distinct MAPK activation profiles. *The Journal of Immunology.* 2026;215:vkag180. DOI PubMed
13. Xie H, Liu H, Xiu Y, et al. Activation of GABABR alleviates colitis by reprogramming macrophage polarization via the IRAK-M/NLRP3/NF-κB pathway. *Biochem Pharmacol.* 2026;252:118227. DOI
14. Tsukamoto H, Takeuchi S, Kubota K, et al. Lipopolysaccharide (LPS)-binding protein stimulates CD14-dependent Toll-like receptor 4 internalization and LPS-induced TBK1-IKKε-IRF3 axis activation. *J Biol Chem.* 2018;293:10186-201. DOI PubMed PMC
15. Sheidae Mehne Z, Honarjou E, Khamoushi Kahdouee M. Chronic infections of the spine: a systematic review of microbial etiologies, diagnostic approaches, and treatment outcomes. *Int J Infect Dis.* 2026;169:108769. DOI PubMed
16. Su GL, Simmons RL, Wang SC. Lipopolysaccharide binding protein participation in cellular activation by LPS. *Crit Rev Immunol.* 1995;15:201-14. DOI PubMed
17. Juffermans NP, Verbon A, Van Deventer SJH, et al. Serum concentrations of lipopolysaccharide activity-modulating proteins during tuberculosis. *J INFECT DIS.* 1998;178:1839-42. DOI
18. Schumann RR. Old and new findings on lipopolysaccharide-binding protein: a soluble pattern-recognition molecule. *Biochem Soc Trans.* 2011;39:989-93. DOI PubMed
19. Futami Y, Takeda Y, Koba T, et al. Identification of CD14 and lipopolysaccharide-binding protein as novel biomarkers for sarcoidosis using proteomics of serum extracellular vesicles. *Int Immunol.* 2022;34:327-40. DOI PubMed PMC
20. Shi Z, Wang Y, Gu Y, Zhu M, Li M, Yu Q. Indolicidin attenuates inflammation by modulating the TLR4 signaling pathway during sepsis progression. *ACS Infect. Dis.* 2026;12:2288-302. DOI
21. Ma Y, Jiang Q. NF-κB signaling in acute myocardial infarction: pathophysiology, inflammation, and therapeutic implications. *Front. Cardiovasc. Med.* 2026;13:1847945. DOI PubMed PMC
22. Zhang Q, Sun J, Fu Y, et al. Guttiferone K Exerts the anti-inflammatory effect on *Mycobacterium tuberculosis*- (H37Ra-) infected macrophages by targeting the TLR/IRAK-1 mediated Akt and NF-*κ*B pathway. *Mediators Inflamm.* 2020;2020:1-16. DOI PubMed PMC
23. Benedetto GL, Parrotta EI, Covello R, et al. Synovial fluid proteomic biomarkers in periprosthetic joint infection: a systematic review with gene ontology and protein network analyses. *J. exp. orthop.* 2026;13:e70853. DOI PubMed PMC
24. Arya R, Shakya H, Chaurasia R, Haque MA, Kim J. Exploring the role of extracellular vesicles in the pathogenesis of tuberculosis. *Genes.* 2024;15:434. DOI PubMed PMC
25. Jain M, Anuja AK, Yadav S, Ara J, Ojha A, Chaturvedi CP. Non-coding RNA in osteoarthritis: mechanistic insights and future perspectives. *Front. Endocrinol.* 2026;17:1851589. DOI PubMed PMC
26. Anderson NL, Anderson NG. The human plasma proteome. *Mol Cell Proteomics.* 2002;1:845-67. DOI PubMed

27. Gabay C, Kushner I. Acute-phase proteins and other systemic responses to inflammation. *N Engl J Med.* 1999;340:448-54. DOI PubMed